Proceedings of the ASME 2011 30th International Conference on Ocean, Offshore and Arctic Engineering
OMAE2011
June 19-24, 2011, Rotterdam, The Netherlands

OMAE2011-50336

DEVELOPMENT OF A NOVEL 1:7 SCALE WAVE ENERGY CONVERTER

Ken Rhinefrank, Al Schacher, Joe Prudell
Erik Hammagren
Columbia Power Technologies, LLC
4920 SW 3rd Street, Suite A
Corvallis, Oregon 97333

Zhe Zhang, Chad Stillinger, Ted Brekken,
Annette von Jouanne, Solomon Yim*
School of Electrical Engineering and Computer Sci.
School of Civil and Construction Engineering*
Oregon State University
Corvallis, Oregon 97331

ABSTRACT
This paper presents a novel 1:7 scale point absorber wave energy converter (WEC), developed by Columbia Power Technologies (COLUMBIA POWER). Four hydrodynamic modeling tools were employed in the scaled development and the optimization process of the WEC, including WAMIT, Garrad Hassan's GH WaveFarmer, OrcaFlex and ANSYS AQWA. The numerical analysis development is discussed, and the performance and mooring estimates at 1:7 scale and full scale are evaluated and optimized. The paper includes the development of the 1:7 scale physical model and the associated WEC field testing in Puget Sound, WA.

1. INTRODUCTION
Ocean wave energy has the potential to be a significant contributor to renewable energy portfolios for many regions in the world. To address this opportunity, COLUMBIA POWER is conducting a comprehensive WEC development program including numerical modeling, scaled wave tank testing and intermediate scale field testing along the path to full scale development. The scaled development process is designed to ensure that energy production and survival characteristics are verified at the earliest and least expensive stages of WEC development.

As part of COLUMBIA POWER's development process, this paper will present the development of a novel 1:7 scale point absorber WEC. Preceding this 1:7 scale WEC, COLUMBIA POWER conducted 1:33 and 1:15 scale testing in the Oregon State University (OSU) O.H. Hinsdale Wave Research Lab (HWRL), in conjunction with the Northwest National Marine Renewable Energy Center (NNMREC). COLUMBIA POWER's 1:33 scale WEC was tested in the directional 3D tsunami wave basin in the fall of 2009 and their 1:15 scale WEC was tested in the 2D large wave flume in the winter of 2010.

This type of scaled "experimental" hydrodynamic analysis provides a cost effective solution to understanding complicated fluid forcing on ocean structures. In broad terms, scaled experimental hydrodynamics retain the complicated hydraulic processes that exist around the system of interest, allow for cheaper and easier quantifiable measurements of relevant criteria or parameters and permits researchers to accurately control incident fluid forcing on models [1]. Also, conditions that are difficult to evaluate analytically or numerically can be included in experimental tests, such as spread spectrum irregular seas, extreme wave heights and slopes or survivability conditions corresponding to long return period sea states. An outline of other considerations for scaled WEC laboratory testing is provided in [2].

When developing a new WEC, the ability to evaluate the impact of significant design changes on the performance of the machine relatively quickly and at a low cost is of pivotal importance. The development of a numerical simulation which is able to address these issues is the typical answer to such a problem. Although there are some similarities with the offshore oil and gas industry in terms of the numerical tools that can be applied, the specific nature of wave energy conversion often requires that custom-made numerical approaches are developed. COLUMBIA POWER has been utilizing four hydrodynamic modeling tools for WEC performance optimization including WAMIT, Garrad Hassan's GH WaveFarmer (a specialized numerical code being developed specifically for the wave energy industry), OrcaFlex and ANSYS AQWA. This paper will include the numerical analysis development and the design optimization for the 1:7 scale WEC, in addition to the planned intermediate scale testing.

2. WAVE ENERGY CONVERTER DESCRIPTION
COLUMBIA POWER's WEC is a point absorber designed to convert both heave and surge wave energy directly into rotary

motion to harness twice the energy of other point absorbers operating solely in heave [3]. The relative surge and heave motions are depicted in Fig. 1. The system converts the heave and surge motion into high torque rotary motion, using direct drive rotary (DDR) generators to provide simple and reliable energy conversion [4-7].

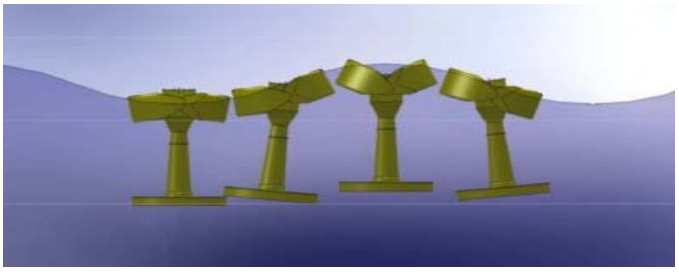

Fig. 1. COLUMBIA POWER's SeaRay wave energy buoy.

The buoy is comprised of three moving bodies; fore float, aft float and spar. The spar is designed to stay relatively stationary in heave by using a large damper at its base. Each float is connected to the top of the spar through a drive shaft. The forward float is connected to the starboard DDR generator and the aft float is connected to the port drive shaft and generator. Normally oriented with the fore float heading into the wave, the incoming heave and surge forces of the waves force the fore float and aft float to rotate about the spar and drive the generator. The approximate full scale diameter is 18 m and draft from surface to the lowest point is 25 m.

3. NUMERICAL MODELING OVERVIEW

Models have been developed for performance and mooring evaluation. GH Wave Farmer is coupled with WAMIT, power takeoff (PTO) loads, WEC mass matrices, inertial matrices and mooring loads to evaluate energy capture performance of the WEC and to optimize its shape.

OrcaFlex was chosen as a hydrodynamic modeling tool for mooring analysis. OrcaFlex is a time domain tool which gives it the capability to model nonlinear mooring arrangements where frequency domain modeling cannot. The model hydrodynamic added mass and damping coefficients are imported from the WAMIT frequency-domain modeling.

ANSYS AQWA is a powerful and flexible hydrodynamic analysis tool that enabled multiple design optimization simulations for the 1:7 scale WEC development.

The following GH and OrcaFlex materials (section 3.1-3.2) were included in the previous paper [5], and are summarized again here for the convenience of the reader and for continuity.

3.1. GH WAVEFARMER MODEL

The GH WaveFarmer software package consists of an equation of motion solver for each specific module: frequency and time domain, respectively. The hydrodynamic properties are loaded from WAMIT. The frequency domain module of GH WaveFarmer allows the calculation of response surfaces which give the average absorbed power as a function of the incident waves field, the PTO damping coefficients and the control strategy. A representative example of relative capture width (RCW) performance is shown in Fig. 2. Plots of this type provide for informed decisions regarding device optimization.

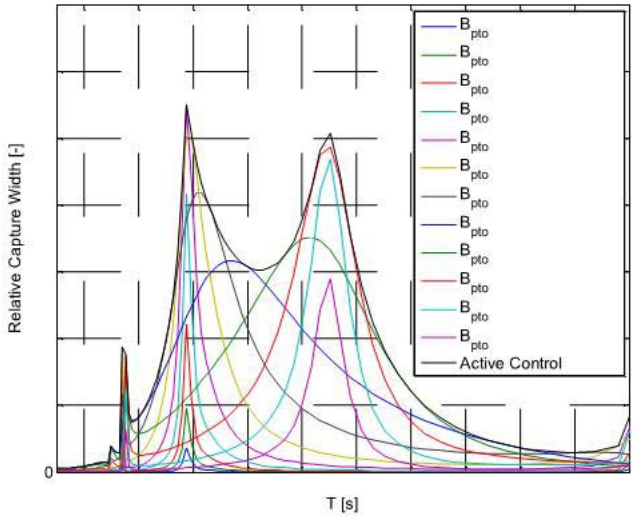

Fig. 2. RCW vs. period (T) and damping (B).

Time domain models were used to perform an initial investigation on the capability of the model. Fig. 3 shows time domain predictions of instantaneous (red) and average (blue) power delivered from the WEC.

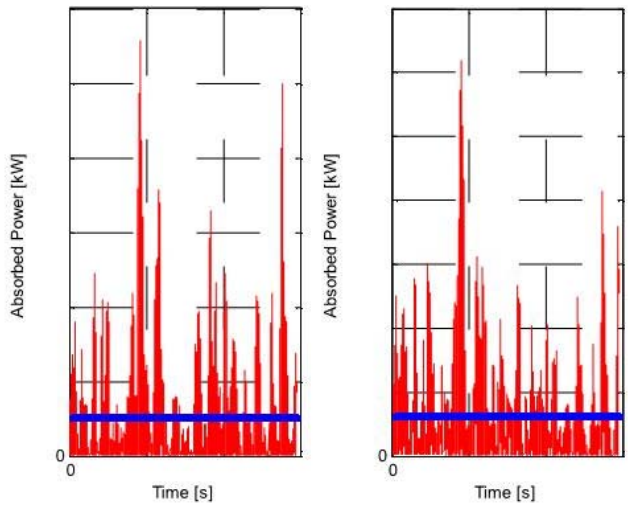

Fig. 3. Fore (left) and Aft (right) time domain power prediction.

3.2. ORCAFLEX MODEL

OrcaFlex is a time-domain numeric solver that gives an intuitive view of how the numerical model correlates to the real world. It provides several connection types for modeling a variety of different mooring systems. With these tools one can

quickly define a variety of connection systems. It also contains a classification of bodies known as 6D Buoy which was initially chosen to model this COLUMBIA POWER SeaRay buoy.

Links were chosen for the connection components to model the real system. Four spring Links were used to model the floats' rotary bearings mounted to the spar, four additional damping Links were used to model the electrical generator damping and 3 Links were used to model the mooring system. Fig. 4 shows the final OrcaFlex model, consisting of three 6D Buoys and eleven Links.

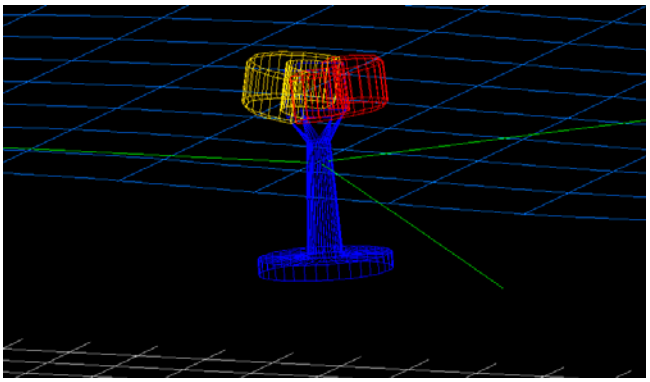

Fig. 4. WEC wireframe in OrcaFlex.

Unfortunately the spring and damper elements are limited to linear motion. Therefore, in order to model rotary damping, i.e., the rotary electric generator, a novel arrangement of linear components is used as shown in fig.5. Details of this conversion are presented in the previous paper [5].

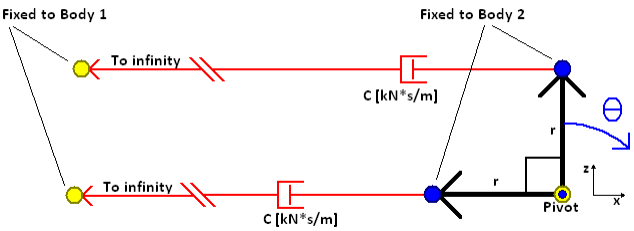

Fig. 5. Diagram of linear to rotary damper arrangement.

3.3. ANSYS AQWA ANALYSIS TOOL

The ANSYS AQWA suite is a set of powerful and flexible hydrodynamic and mooring analysis tools that enabled multiple design optimization simulations for the 1:7 scale WEC developments. The AQWA suite contains six programs, as shown in Fig. 6, and is capable of performing radiation/diffraction, equilibrium/stability, frequency domain, and time domain analyses [8].

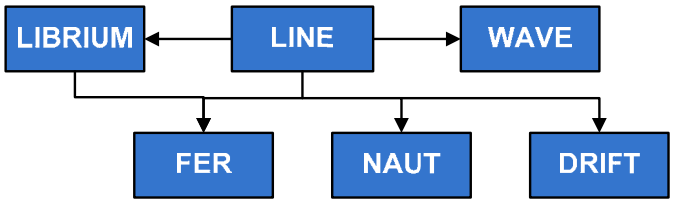

Fig. 6. AQWA programs.

AQWA-FER is a frequency domain program to analyze structure motion for wave frequency (first order force) and/or drift frequency (second order force) with mooring tension, currents and wind in irregular waves. It takes both results from LINE (linearized hydrodynamic fluid wave loading) and LIBRIUM (static equilibrium configuration) to start off, and outputs RAOs of each structure and mooring tensions. Damping at each articulation axis can be used as PTO forces. Combining relative RAOs with damping settings, RCW performance analysis as shown in Fig. 2 can be done during the post-process.

AQWA-NAUT and AQWA-DRIFT are the time domain counterparts of FER. In NAUT, non-linear hydrostatics and Froude-Krylov forces are computed with instantaneous wetted surfaces. Second order drift forces are omitted, but with some second order effects. As for DRIFT, unlike NAUT, only linear hydrostatic stiffness is computed with mean wetted surfaces, however, second order drift coefficients are included. The selection between these two time domain programs is dependent on the application. For this WEC, due to the large range of motion and the size of the device, instantaneous wetted surfaces and non-linear forces are needed to compute accurate results. Therefore, NAUT was selected to use during the design process. Another feature of these two time domain programs is external force input. For each time step, 6 DOF forces and an added mass matrix for each structure can be applied to the simulation via a dynamic-link library (dll). This feature enables interactions between AQWA and other programs such as MATLAB. In the generator control development of this WEC, MathWorks Simulink was used to compute generator effects and then the results were used as feedback to AQWA-NAUT simulations. The final results can then be processed into mechanical power, as shown in Fig. 3, as well as electrical power outputs when in knowledge of gear and generator characteristics.

4. PERFORMANCE AND MOORING ESTIMATES

Performance and mooring estimates at 1:7 scale and full scale are evaluated and optimized.

4.1. PERFORMANCE EVALUATION

To evaluate the performance of WEC shapes, mass matrices, damping values, and torque limits, results from AQWA simulations are processed into charts such as important RAOs, RCW, mechanical power, and power ratios. The same process was also used to simulate the effects of mooring arrangements,

directionality, making performance predictions and the process assisted in making COE estimates. The entire process includes five parts from RAOs in AQWA-FER to energy predictions.

4.1.1. RAOs from AQWA-FER

AQWA-FER provides frequency dependent RAOs for each structure in the heave, surge, sway, pitch, yaw and roll directions. The RAOs provide magnitude and phase data for each structure and every damping setting based on a one meter amplitude regular wave input. RAOs are then processed into the relative velocities and torques between floats and spar. Scaling these per meter RAOs by wave height provides all the needed data for power calculation. The best damping case for each period of peak spectral energy (T_p) and significant wave height (H_s) are systematically selected to produce an active control map, described in section 4.1.5. The RAOs resulting from the active control includes pitch, heave, relative velocities and torque. Among these, there is an important phase relationship that is of interest: the phase difference between the floats' pitch and spar's heave as shown in Fig. 7.

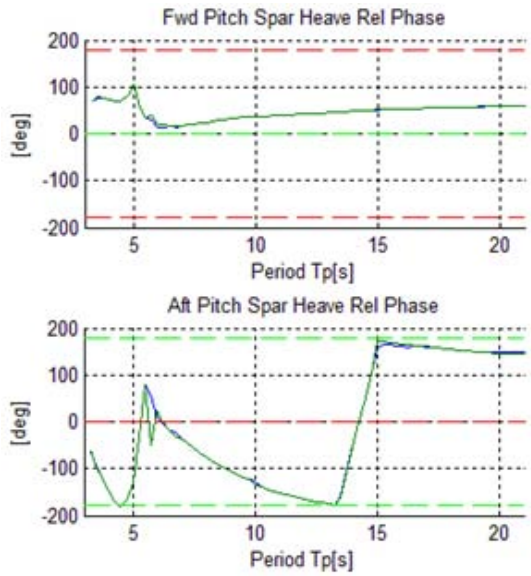

Fig. 7. Relative phase between floats' pitch and spar's heave.

These two plots indicate whether the pitch of the floats and the heave of the spar are in-phase or out-of-phase respectively. Ideally, both floats would be out-of-phase with the spar to obtain maximum velocity at articulation points. The desired out-of-phase relationship is shown as the dashed green guide line, while the in-phase relationship is in red. The guide lines are switched between the Fore and Aft floats due to the sign convention between their rotations.

Fore and Aft damping settings are swept through 6 values to create a 6x6 matrix for a total of 36 damping combinations. WEC performance for each of the 36 damping cases (*damp*) is simulated in AQWA for *Hs* and *Tp*.

A torque limit is imposed on the torque RAOs in order to represent a physical limit of the direct drive generator. Data taken from tank testing was used to generate a plot of the average power level versus an imposed torque limit that was swept for all winter wave climates. Fig. 8 shows an example of this average power versus maximum torque (*Tmax*) plot showing the *Tmax* value at the transition point in the curve; all climates showed similar results. The maximum damping value is based on generator efficiency limits, resulting in an ω_{Tmax} at which *Tmax* is achieved.

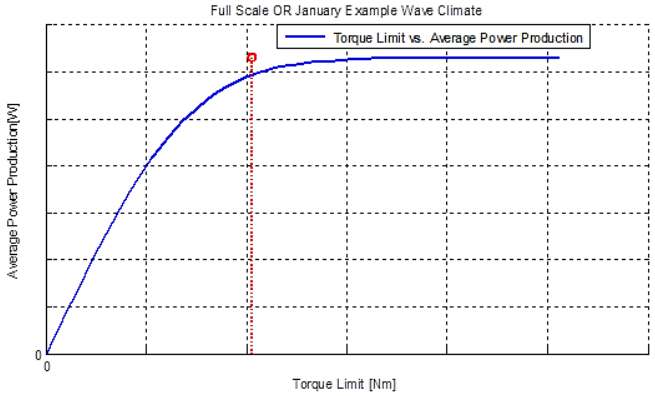

Fig. 8. Average power versus imposed torque cap Example.

The torque RAOs [*Nm/m*] are multiplied by the wave height axis values in order to generate a four-dimensional table of Torque (*H,T,damp*) in units of [*Nm*]. This creates torque values which exceed the direct drive maximum torque capabilities. To overcome this discrepancy the values from the torque table were limited to T_{max}.

4.1.2. Power Calculations

The first rough estimations of both WEC mechanical power output and wave power are computed and used for the regular wave RCW calculations described in section 4.1.3.

WEC power (P_{WEC}) is calculated directly from RAO values of relative velocities and torques. Each RAO based on a one meter amplitude input wave modeled in AQWA is multiplied by the wave height axis to give 4D RAO's based on *T*, *H*, and damping. For WEC power predictions, a torque limited 4D torque RAO is used. Since RAO values are peak values, each is divided by $\sqrt{2}$ to give RMS values.

$$P_{WEC_{regular}}(T,H,damp) = \frac{\tau_{RAO}(T,H,damp)}{\sqrt{2}} * \frac{\omega_{rel}(T,H,damp)}{\sqrt{2}} \quad (1)$$

The intermediate water depth regular wave power equation is used to compute the power from the input wave. The wave power is calculated at a desired water depth (*h*), the same water depth used in AQWA-LINE. The wave power is solved for each period and wave height creating a 3D wave power table at this water depth.

$$P_{WAVE_{regular}}(T,H) = \frac{1}{8}\rho g * c_g(T,h) * H^2 \quad (2), [9]$$

4.1.3. RCW Computation

A family of Relative Capture Width curves is calculated for each of the 36 PTO damping cases. For comparison, two distinct RCW families are computed. One uses unlimited values for torque and the other having the direct drive generator torque limit to show the potential mechanical power output gain.

For RCW without torque limit, the WEC power is first divided by the width of the WEC for the power per meter width. In the unlimited torque case the wave height does not affect the RCW curve since H^2 is in both the numerator and denominator. Therefore the regular wave RCW calculation can be written in terms of only T and damping:

$$RCW_{regular}(T, damp) = \frac{P_{WEC\_regular}(T,damp)}{P_{wave\_regular}(T)*Width} \quad (3)$$

Frequency domain modeling assumes torque increases linearly with wave height. However, PTO torque limits must be considered for energy predictions. The torque limited RCW is defined based on the 4D torque limited RAOs. This torque limited RCW is used for all subsequent power and energy calculations.

$$RCW_{T\_Limited}(T,H,damp) = \frac{P_{WEC\_T\_Limited}(T,H,damp)}{P_{wave\_regular}(T,H)*Width} \quad (4)$$

4.1.4. Wave Power Spectrum

A wave power spectrum based on a Pierson-Moskowitz energy spectrum is calculated for each wave climate (*Hs*, *Tp*) based on the water depth at the specific geographic location. Combined with the RCW computed from the last section, more accurate estimations of WEC power than that from section 4.1.2 can be calculated.

A three-dimensional table of spectral energy data is created for each wave climate based on *Hs* and *Tp*. This table is of the same dimensions as the Occurrence Table defined later in section 4.1.4. The energy spectrum $s(T_p, H_s, f)$ $[\frac{m^2}{Hz}]$ is derived from the two parameter Pierson-Moskowitz equation:

$$\boldsymbol{s(T_p, H_s, f) = A(\frac{1}{f})^5 * \exp(-B(\frac{1}{f})^4)} \quad (5), [10]$$

where $A = \left(\frac{1}{2}H_s^2\right) * B$ and $B = \frac{5}{4}(T_p)^{-4}$

Group velocity (c_g) is a water depth (h) dependent value and must be recomputed for every wave climate. It describes the rate that wave energy is transmitted by the wave and is computed as following:

$$c_g(f,h) = \left[\frac{1}{2} + \left(\frac{kh}{\sinh(2kh)}\right)\right] * c(f,h) \quad (6), [9]$$

where $c(f,h) = \frac{gT}{2\pi}\tanh(kh)$

k is solved from: $(2\pi f)^2 = gk * \tanh(kh)$

With the knowledge of $s(T_p, H_s, f)$ and c_g, power from the wave spectrum for every H_s, T_p and h can then be computed, which is used for all subsequent calculations.

P_{wave} [W/m]: $J = \rho g \int_0^\infty c_g(f) * s(f)\, df$ (7), [10]

Finally, the average power absorbed by the WEC (P_{WEC_spec}) in the new estimation is ready to be computed for every H_s, T_p, h and damping.

$$P_{WEC\_spec} = Width * \rho g \int_0^\infty [c_g(f) * s(f) * RCW_{T\_Limited@Hs}(f)]\, df \quad (8)$$

where $RCW_{T\_Limited@Hs}$ is the torque limited RCW at H_s as shown in Fig. 9. The spectrum period (T) in this figure is then converted to frequency (f) for integration in the above equation (13).

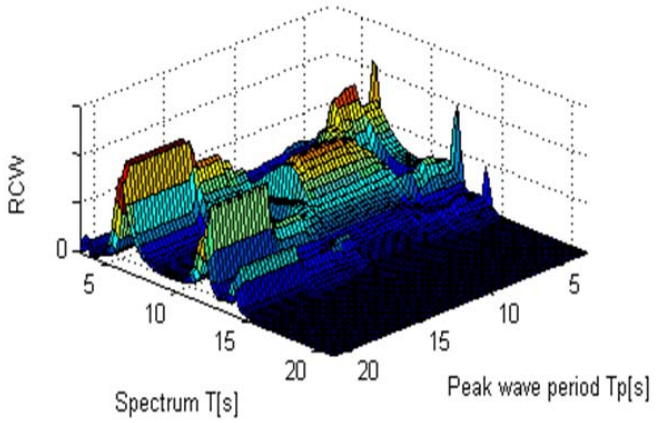

Fig. 9. Torque limited RCW at *Hs* for every T_p and *T*.

The average power levels are compared and the damping case that provided the highest average power level is chosen as the active damping setting for each *Tp*, *Hs* and water depth (*h*).

4.1.5. Energy Predictions

To calculate annual energy estimation for each wave climate, the occurrence table is used. This is a statistical representation of wave data that lists the number of hours per year that each wave condition (*Hs*,*Tp*) occurred in a given wave climate. Fig. 10 shows an example of the Oregon wave climate, plotted with the annual energy in the color scale.

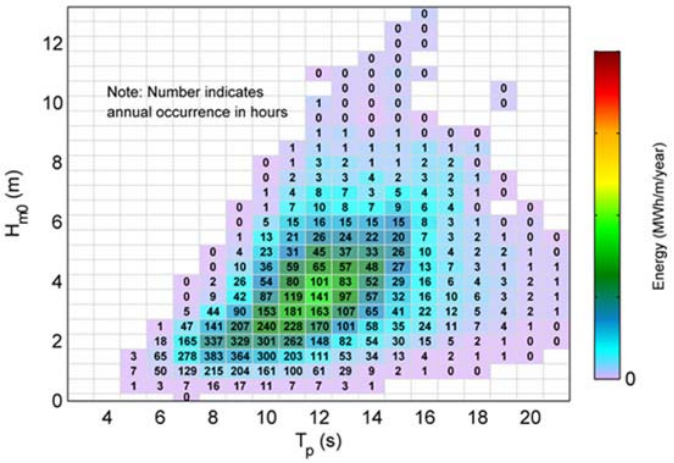

Fig. 10. Oregon Occurrence Table: Color scale [MWh/m/year], number indicates annual occurrence [hours].

The total annual energy is calculated by multiplying the active power for each *Tp* and *Hs* with the number of hours each *Tp* and *Hs* occurred annually provided in the occurrence table. This creates an energy table representing the total energy produced by each *Tp* and *Hs* annually, seen in Fig. 10 in the color scale. This table is then summed with a double integral into a single number representing the estimated energy produced from the given wave climate.

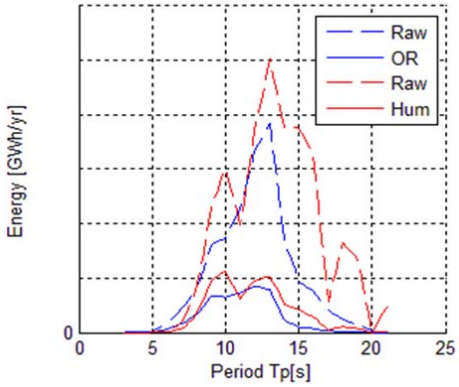

Fig. 11. Examples of E_{WEC} and E_{wave} for two wave climates.

By taking a single integral of the energy table in the *Hs* direction we get a 2D spectral energy curve representing an annual estimate of total WEC absorbed energy (E_{wec}) for each dominant period *Tp*.

$$E_{WEC}(T_p, h) = \int [E_{WEC}(H_s, T_p, h)]\, dH_s \qquad (9)$$

A similar summation can be made with the raw wave energy in a given wave climate resulting in a curve estimating energy per *Tp*.

$$\boldsymbol{E_{wave}(T_p, h) = \int [E_{wave}(T_p, H_s, h)] dH_S} \qquad (10)$$

These two spectral energy curves are computed for each of the wave climates that are being investigated as shown in Fig. 11. In the figure, dot lines labeled as raw is E_{wave}, while solid lines represent E_{wac}.

Having both the spectral WEC absorbed energy and spectral raw energy which the WEC was exposed to, we are able to define a Power Ratio on the spectral axis for each wave climate as shown in Fig. 12.

$$Power\_Ratio(T_p, h) = \frac{E_{WEC}(T_p,h)}{E_{wave}(T_p,h)} \qquad (11)$$

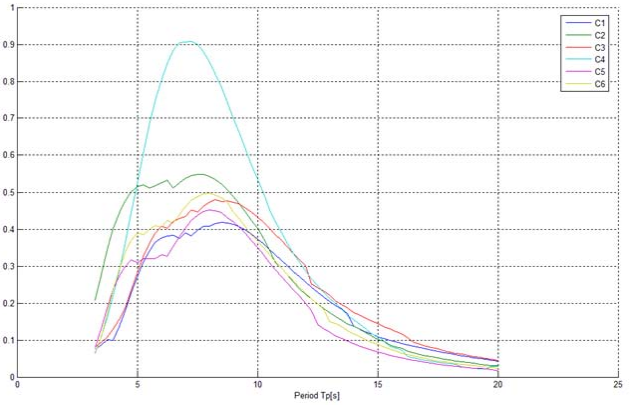

Fig. 12. Power ratios of six different shapes in a selected wave climate.

Since both the numerator and denominator are products of the Occurrence Table the calculation is equivalent to a power ratio, thus the name. Power Ratio is a unit-less term giving an indication of the WEC's ability to absorb power. Power Ratio is symbolic of the WEC capture efficiency over the spectra.

4.2. TIME DOMAIN PERFORMANCE

As mentioned in section 3.3, AQWA-FER is a frequency domain program, which is fast in terms of computing speed compared to time domain programs like NAUT and DRIFT. This makes it ideal for the shape optimization process since it requires a large number of simulations and geometry changes. Yet, there are three issues with using FER. First, in the frequency domain, non-linear effects cannot be included. Second, the generator control approach is limited. Last, actual electrical power output cannot be computed. These three drawbacks lead to the generator control optimization process to be conducted in the time domain. All generator effects are computed in Simulink and then fed back to AQWA-NAUT for every time step. Four generator control algorithms were optimized for five typical Oregon sea states: linear damping, square wave torque, clipped reactive and soft latching.

4.2.1. SIMULATION SETUP

Software is developed around AQWA-NAUT to perform time domain simulations with non-linear generator effects computed in MathWorks Simulink. A custom Microsoft Windows-based program (Main GUI block in Fig. 13), written in C# automates the simulation and data post-process. This

dialog based application allowed simulation parameters to be selected that directed the simulation process such as sea state, type and settings of generator control algorithm, simulation period, time step size etc. This program generates a task list based on a defined range of generator control settings from the graphical user interface (GUI). The task list then gets stored in a data base with associated settings, which is used to initialize each time domain simulation in AQWA-NAUT. AQWA time integration is based on a 2-stage predictor corrector method. During the simulation, an external force routine (user_force.dll as shown in Fig. 13) is therefore called twice at each time step. This external force represents the generator torque based on the various simulation results, which is fed back to AQWA-NAUT. All intermediate results are stored back to the data base, which are post-processed into the time history profile of mechanical power output, electrical power output and generator efficiency.

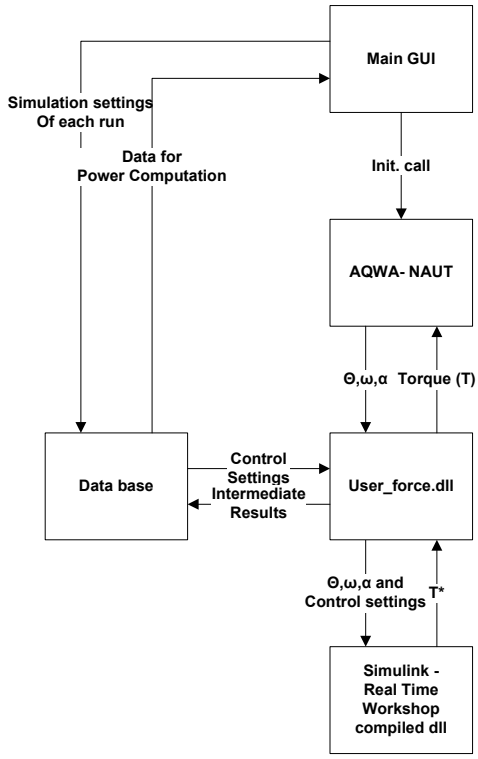

Fig. 13. Time domain simulation setup.

dSPACE is used on the 1:7 buoy as the control hardware. The main advantage of this setting is the generator control block in Simulink can be directly used in dSPACE, which means the generator control system during the simulation is exactly identical to the one on the actual buoy. This minimizes possible error during the transition from simulation to implementation.

With performance measurements in terms of average electrical power output, generator control settings can be optimized as shown in Fig. 14. In this figure, the performances of soft latching with different settings are plotted. The optimal control setting is then selected.

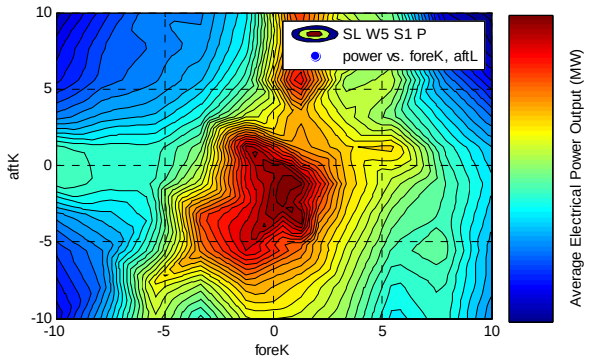

Fig. 14. Performances of soft latching with various settings in a selected sea states.

4.2.2. GENERATOR CONTROL ALGORITHMS

Linear damping and square wave torque are simple and straight forward. For clipped reactive, torque is used to act as stiffness (K) and the moment of inertia (M) of the floats.

$$T^* = K\theta + B\dot{\theta} + M\ddot{\theta} \qquad (12)$$

If instantaneously the commanded torque T* is of opposite sign of $\dot{\theta}$, then T* is set to zero. This prohibits the generator from putting power back into the ocean. The difficulty of optimizing this control approach is the number of variables. A total of six variables needs to be optimized for both fore and aft generators. A linear sweep over this 6-D space is time costly. Therefore, a particle swarm search algorithm was implemented to effectively search this space as shown in Fig. 15. In this figure, 2D (Fore B and Fore M) out of six are selected for plotting, each line represents the movement of a particle. There are a total of $16 = 2^4$ particles placed to cover 4 boundary conditions: fore B, fore M, aft B and aft M.

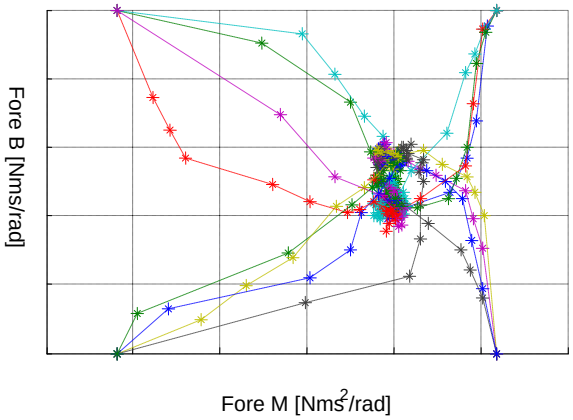

Fig. 15. Movements of particles.

Let each set of six variables be $\underline{P}$ and last movement be $\underline{V}$, then the particle swarm optimization algorithm is defined in

the following for this application. For the next step of n^{th} particle:

$$\underline{V}_{(n,t+1)} = \underline{m} * \underline{V}_{(n,t)} + a_g * \underline{v}_g * \left(\underline{P}_{(global\_max,t)} - \underline{P}_{(n,t)}\right) + \underline{v}_l * \left(\underline{P}_{(local\_max,t)} - \underline{P}_{(n,t)}\right) \quad (13)[11]$$

$$\underline{P}_{(n,t+1)} = \underline{P}_{(n,t)} + \underline{V}_{(n,t+1)}$$

where

a_g is global acceleration:

$\lim_{t\to 0} a_g = a_{g_0} = 0.5$ and $\lim_{t\to t_f} a_g = 1$

$\underline{v}_g$ and $\underline{v}_l$ are global velocity and local velocity, uniformly distributed random values from 0 to 0.2

$\underline{m}$ is momentum, which is set to 0.05

$\underline{P}_{(global\_max,t)}$ is the location of maximum fitness of all particles

$\underline{P}_{(local\_max,t)}$ is the location of maximum fitness of n^{th} particle

Though this algorithm does not guarantee to find the global maximum, it is able to find one of the local maximum points within ten iterations as shown in Fig. 16.

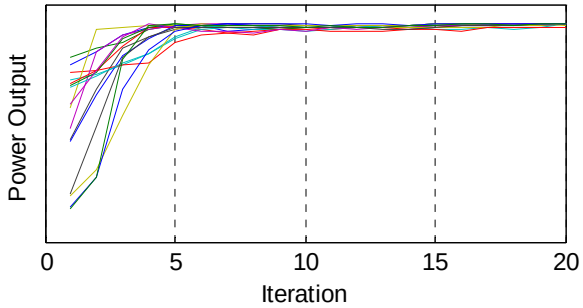

Fig. 16. Performance of each particle in terms of average electrical power output.

The soft latching approach mimics a latching action by controlling generator damping (*B*), since there is no physical device to perform the actual latching action.

$$B = \begin{cases} B_{opt} * b^{\left(-k\left(\frac{\theta}{\theta_{end}}\right)\right)} & , \ \dot{\theta} \geq 0 \\ B_{opt} * b^{\left(k\left(\frac{\theta}{\theta_{end}}\right)\right)} & , \ \dot{\theta} < 0 \end{cases} \quad (14)$$

The base b can be selected to be any value, the same being valid to k. To simplify the optimization process, base b is fixed and only the value k can be varied. The end stop location θ_{end} is the range of motion for each float.

4.3. MOORING ESTIMATES

Mooring design is a vital component of the overall design process for survivability of the device, as well as for the performance. The mooring system was designed to be capable of surviving 100 year storms with a life expectancy of 20 years. Fig. 17 shows a snapshot of the mooring design during the time domain simulation.

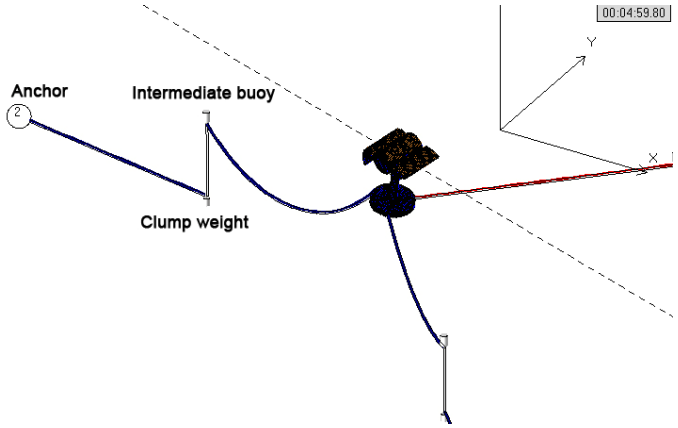

Fig. 17. Mooring system in the time domain simulation.

The mooring system affects the overall performance in terms of yaw stability. This WEC is designed to achieve maximum efficiency when the dominant wave direction is head-on. Any yaw instability can potentially reduce WEC power output. Fig. 18 shows an example performance comparison with different dominant wave directions. The head-on wave direction is used as a base line case. This result varies in different sea states, wave spreading patterns and other environmental conditions, but it mostly follows the same trend with exceptions in some extreme conditions.

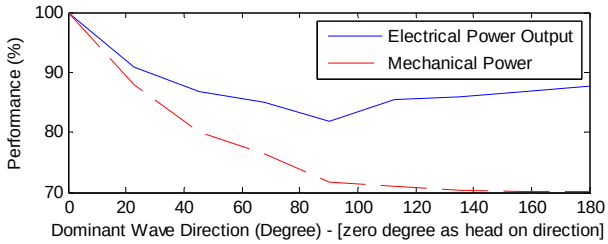

Fig. 18. WEC performance vs. dominant wave direction.

5. 1:7 SCALE PHYSICAL MODEL DEVELOPMENT

Since the original manta shape (Fig. 1), there has been significant improvements on the shape, mass matrices, location of the center of gravity and inertia matrices to increase WEC performance. The baseline geometry is the exact full scale representation of the 1:15 scale. A validation process was conducted to align the numerical model in AQWA with the 1:33 scale tank test results to ensure the accuracy of the simulation. This validation process includes RAO comparisons of every direction for each structure in the frequency domain. Fig. 19 shows the comparison in the heave direction of the spar. The 250 kN/m external spring force is added to mimic the data cable on the 1:33 scale buoy. The viscous effect on different scale buoys also causes the difference between the AQWA results and the tank test results.

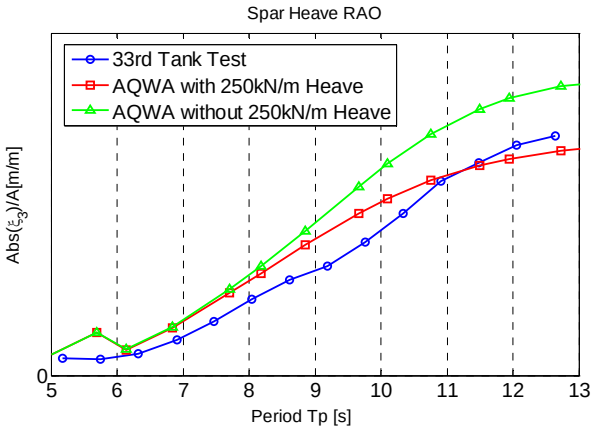

Fig. 19. Validation of simulation models in spar heave.

Once the validation process was completed, a list of physical changes to the WEC that are hypothesized to have an effect on the WEC performance was collected. Each hypothesis was then explored to determine potential benefits to WEC performance and to provide a physical understanding of the change through the process described in section 4.1. This hypothesis list was prioritized by importance based on changes that are expected to have the largest performance gains, and it was constantly updated as the optimization process proceeded.

In addition to performing optimization using the hypothesis list for mass matrices, the location of the center of gravity and inertia matrices, optimization was also performed using neural network (NN) methods. The resulting match between the methods was very encouraging.

6. FIELD TESTING IN PUGET SOUND.

At the time of this paper submittal, COLUMBIA POWER is in the process of field testing their 1:7 scale WEC in Puget Sound, WA (winter – spring 2011). Besides tests of hardware implementations such as the SCADA system and remote control, three important goals for this field test include 1) the validation of frequency domain power estimation with linear damping, which is used during physical model development (section 4.1 & 5.0), 2) the validation of performance in different sea states with varied control algorithms, which is used during the generator control optimization (section 4.2), and 3) survivability and reliability, which includes predicted loads and survival assumptions. The difference between previous numerical simulations and this field test will determine the direction of further research.

Puget Sound was selected for the scaled WEC testing due to the wave climate (the wind waves are a good match for the 1:7 scale WEC), in addition to the water depth and the facility accessibility. The site is in the scale range of 1:10 to 1:5, which is determined by scaling the occurrence table of testing period to match the full scale sea climates. There are two conditions that do not match after scaling: tidal variation and currents. Both are much larger after scaling than the full scale wave climate.

Five typical Oregon west coast sea states are selected to represent the rest of Oregon's wave climate. For each sea state there is a priority list of tests that needs to be completed. Each list contains varied generator control approach settings. There is also an active yaw control device on this scaled WEC to validate the effects of yaw stabilization.

7. CONCLUSIONS

This paper presented the development of a novel 1:7 scale point absorber wave energy converter (WEC). The WEC was developed by Columbia Power Technologies (COLUMBIA POWER), in research collaboration with Oregon State University (OSU). The numerical analysis development is presented, employing four hydrodynamic modeling tools, and the performance and mooring estimates at 1:7 scale and full scale are evaluated and optimized. The paper includes the development of the 1:7 scale physical model and the associated WEC field testing in Puget Sound, WA.

8. ACKNOWLEDGEMENTS

The Columbia Power Technologies' SeaRay WEC is being developed through collaboration with the following organizations: Oregon State University, Ershigs Inc., Crescere Marine Engineering, Sound and Sea Technologies, Garrad Hassan and Glosten Associates. The depth of knowledge and experience brought into the program through these organizations is highly regarded by the COLUMBIA POWER team.

Funding for this project was from the US Department of Energy and the US Navy administered by Naval Facilities Engineering Command (NAVFAC). Private funding is from Columbia Power Technologies. The authors sincerely thank and appreciate the funding and support to develop this technology and our sponsors' efforts toward achieving pollution free renewable energy sources.

9. REFERENCES

[1] S. A. Hughes, "Physical Models and Laboratory Techniques in Coastal Engineering", World Scientific Advanced Series on Ocean Engineering – Volume 7, 1993, ISBN 981-02-1540-1.
[2] J. Cruz, "Ocean Wave Energy: Current Status and Future Perspectives", Springer Series in Green Energy and Technology, 2008, ISBN 978-3-540-74894-6.
[3] K. Budal, J. Falnes, "A resonant point absorber of ocean-wave power", Nature, vol. 256, Aug. 7, 1975, p. 478, 479.
[4] K. Rhinefrank, J. Prudell, A. Schacher, "Development and Characterization of a Novel Direct Drive Rotary Wave Energy Point Absorber", MTS–IEEE Oceans Conference Proceedings, 2009.
[5] K. Rhinefrank, A. Schacher, J. Prudell, J. Cruz, N. Jorge, C. Stillinger, D. Naviaux, T. Brekken, A. von Jouanne, D. Newborn, S. Yim, D. Cox, "Numerical and Experimental Analysis of a Novel Wave Energy Converter", OMAE, Shanghai, China, June 2010.
[6] K. Rhinefrank, A. Schacher, J. Prudell, C. Stillinger, D. Naviaux, T. Brekken, A. von Jouanne, D. Newborn, S. Yim, D. Cox, "High

Resolution Wave Tank Testing of Scaled Wave Energy Devices", OMAE, Shanghai, China, June 2010.
[7] K. Rhinefrank, A. Schacher, J. Prudell, Chad Stillinger, David Naviaux, Ted Brekken, Annette von Jouanne, "Scaled Wave Energy Device Performance Evaluation through High Resolution Wave Tank Testing", Oceans 2010, September 2010.
[8] ANSYS, 2010. ANSYS AQWA. Available at: http://www.ansys.com/products/aqwa/default.asp [Accessed December 29, 2010].
[9] R.G. Dean, R.A. Dalrymple, "Water Wave Mechanics for Engineers and Scientists", World Scientific, Singapore, 1991, p. 97, 98.
[10] J. Falnes, "A review of wave-energy extraction", Marine Structures, vol. 20, 2007, p. 185-201.
[11] J. Kennedy, R. Eberhart., "Particle Swarm Optimization", Proc. IEEE Int'l. Conf. on Neural Networks IV:1942-1948.